Rapid Report

Single channel currents at six microsecond resolution elicited by acetylcholine in mouse myoballs

Franz Parzefall, Robert Wilhelm, Manfred Heckmann and Josef Dudel

Institut für Physiologie der Technischen Universität München, Biedersteinerstrasse 29, D-80802 Munich, Germany

(Received 2 April 1998; accepted after revision 27 July 1998)

1. A patch-clamp set-up was optimized for low noise and high time resolution. An Axoclamp 200B amplifier was modified to incorporate a Teflon connector to the electrode. An electrode puller was equipped with a hydrogen–oxygen burner to produce quartz-glass pipettes with optimally 0·2 μm openings and 20 MΩ resistance.

2. The r.m.s. (root mean square) noise of sealed pipettes in the bath ranged from 3·6 fA with 100 Hz filter cut-off to 1·5 pA with 61 kHz filter cut-off. At these extremes currents of 17 fA and more than 3 ms, or 9 pA and more than 6 μs could be resolved with a negligible error rate.

3. The system was tested on mouse myoballs, recording 9–10 pA single channel currents on-cell at −200 mV polarization which were elicited by 0·1–5000 μM acetylcholine (ACh).

4. Distributions of open and closed times and of correlations of open times to the preceding closed time defined several open states: single openings with mean durations of 1·2 and 25 μs, from single-liganded receptors, and bursts of 10 ms mean duration containing on average 800 μs openings and 16 μs closings, from double liganded receptors. Above 0·1 mM ACh these openings are interrupted increasingly by on average 18 μs and 72 μs channel blocks by ACh.

Patch-clamp currents allow the observation of conformational changes of single ion-channel molecules. While effective shifts of the membrane potential need current flow of the order of milliseconds, many channels switch to the open or closed states for much shorter times, often for less than 50 μs. These rapid fluctuations contain information about the control of channel opening and closing, but cannot be resolved adequately with normal patch-clamp recordings. For instance in the most studied channel type, the nicotinic receptors of vertebrate muscle, the seminal paper of Colquhoun & Sakmann (1985, Table 5) clarified that the long openings arising from the doubly liganded receptor (Magleby & Stevens 1972) were indeed bursts of on average 1·4 ms openings alternating with 33 μs closings. The highest cut-off filter frequency in this study was 5 kHz, which corresponds to opitimally resolvable open or closed times of about 70 μs. The on average 20 μs closings could be estimated only from distributions of closed times, extrapolating from the shortest exponentionally declining component. These bursts of openings are further interrupted by acetylcholine (ACh) at higher concentrations blocking the open channel (Neher & Steinbach 1978; Sine & Steinbach 1987; Colquhoun & Ogden 1988). The durations of the closings resulting from open channel block could only be estimated by noise analysis or from average currents (Colquhoun & Ogden 1988; Maconochie & Steinbach 1998). Therefore, for this channel type, but also for others, patch-clamp recordings with better time resolution are highly desirable. The quest for a higher time resolution is equivalent to reducing the current noise seen at a specific bandwidth. A reduction of the noise at high bandwidth optimizes also low noise recordings at low bandwidth and improves resolution in the case of single channel currents below 1 pA.

Systematic efforts to increase recording bandwidth or to reduce noise were undertaken by Benndorf (1995), and Levis & Rae (1993) introduced quartz pipettes for this purpose. In the present study we show a further optimization employing quartz pipettes drawn with a newly developed puller as well as low noise amplifier inputs.

METHODS

Following decapitation, the toe muscles of neonatal mice were prepared and the myotubes were cultured for 10 days (Franke *et al.* 1992). The experiments were performed in accordance with national guidelines and care was taken that animals did not suffer unnecessarily. The cultured myotubes expressed only the

embryonic type of nicotinic receptor with a slope conductance of 46 pS measured in cell-attached mode. The extracellular solution (and that in the pipette tip, with ACh added) contained (mM): 162 NaCl, 5·3 KCl, 2 $CaCl_2$, 0·67 NaH_2PO_4, 15 Hepes buffer and 5·6 glucose; the pH was 7·4 (adjusted with NaOH) and bath temperature was 21 °C. Patches were formed in the on-cell mode (Hamill *et al.* 1981). Most measurements were at membrane polarizations of −200 mV with 9–10 pA channel current, in order to increase resolution (resting potential, −30 to −60 mV).

The measured current data were filtered with a ten pole Bessel filter at 78 kHz, digitized at 333 kHz and stored directly on the hard disk of a Pentium Pro computer. The combination of the 78 kHz external filter with the internal 100 kHz filter of the amplifier resulted in a −3 dB cut-off frequency of 61 kHz. Evaluation of the data was achieved with the newly developed X-Patch program running under Unix.

Recording resolution of single channel currents is limited by noise, by rapid current fluctuations generated by the biological current source and by surrounding extraneous sources, especially the apparatus of measurement. In our attempt to reduce the noise we were guided by the study of Benndorf (1994, 1995). The best low noise instrument currently available to measure patch clamp currents is the Axopatch 200B amplifier (Axon Instruments) with a cooled input stage and capacitative feedback. Its standard pipette holder, however, is far from optimal. The long wire contacting the patch pipette is an effective antenna for extraneous electromagnetic fields, and the polycarbonate material of the holder generates unacceptable dielectric losses. We therefore constructed a Teflon connector largely contained in the metal case of the input stage (Fig. 1*A*). The chloride-coated silver wire contacting the electrode tip was soldered directly to the input transistor. The connector fixed a pipette of about 10 mm length filled at the tip with extracellular solution for less than 1 mm (Fig. 1*A*). This brought the head stage very close to the preparation, which was fixed in a chamber on an inverted Zeiss microscope (Axiovert 35), and illumination had to be shifted to a light guide fixed to the head stage (Fig. 1*A*). With this connector and an electrode held just above the recording chamber the noise was reduced to the level of the open amplifier input, i.e. to about 55 fA r.m.s. (root mean square) read from the 5 kHz filtered output of the amplifier.

Pipettes from the usual borosilicate glass produce substantial noise. The main source being the film of salt solution creeping up the wall of the pipette. The suggested coatings (Levis & Rae, 1993; Benndorf 1995) are cumbersome and not fully effective. Quartz glass pipettes have a hydrophobic surface and do not support the creeping of fluid films. Compared with borosilicate glass, quartz has superior electrical characteristics which reduce the input capacity of the pipette. The capacity is optimal when thick-walled glass is used. Quartz has the disadvantage of a high melting point of 1580 °C, and the commercially available laser quartz-electrode pullers cannot provide enough heat to produce thick-walled quartz pipettes. We therefore converted a DMZ puller (Zeitz Instruments, Munich, Germany), replacing the heating coil by a hydrogen–oxygen burner. The gas mixture was generated on-line by water electrolysis in a Hydromat 5000E soldering device (Flume Technik GmbH, Essen, Germany). The gas pressure was regulated and the flow was switched by magnetic valves controlled by the puller program. Pipettes were pulled automatically from 2 mm tubes with 0·5 mm walls, in three stages to achieve a short tapering of the tip. Pipettes with about 20 MΩ input resistance and about 0·2 μm openings proved to be optimal (Fig. 1*B*). In these pipettes the 2 : 1 ratio of the outer to inner diameter of the 2 mm tubes increased to 2·4 : 1 at the tip, reducing the input capacity. In electrodes with a long taper the ratio is below 2.

The r.m.s. noise values achieved with filter cut-off frequencies (f_c) of 100 Hz to 100 kHz are plotted in Fig. 1*C* (circles). A quartz electrode was sealed pushing it into the Sylgard-coated bottom of the recording chamber. The noise is the same as with a good

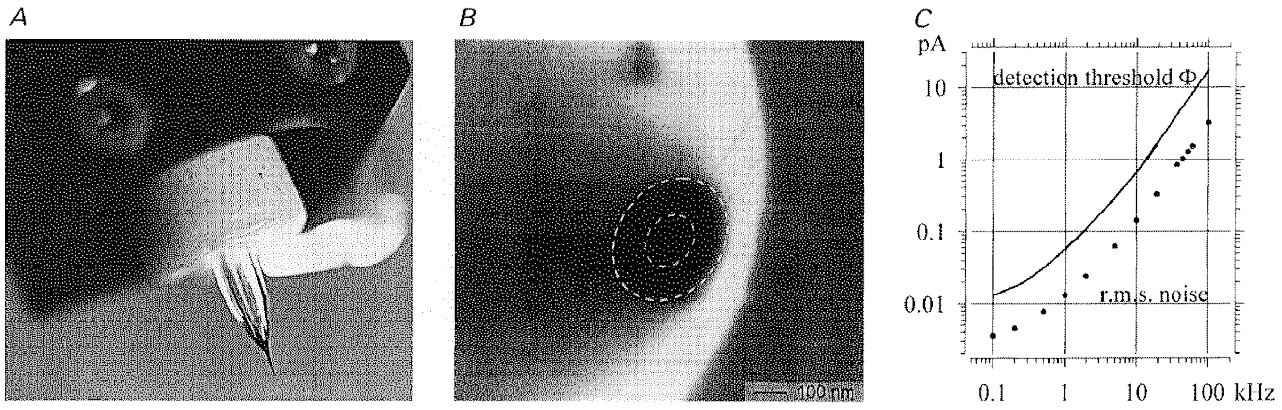

Figure 1. Recording set-up and detection threshold

A, amplifier headstage with 2 mm diameter electrode fixed in an extremely short Teflon connector. A light guide is fastened to the right side of the head stage and feeds into the electrode. The solution in the electrode tip is coloured to demonstrate its low level and to improve the visibility of the electrode tip. *B*, tip of a typical quartz pipette imaged by a raster electron microscope, viewed at about 45 deg. The diameter of the tip is about 410 nm and that of the opening about 170 nm. The diameter of the pipette is seen to increase steeply with distance from the opening, and this seems to result in the relatively low resistance of the sister pipette of 17 MΩ. *C*, r.m.s. noise (circles) measured at the filter cut-off frequency, f_c (abscissa), for a quartz electrode pushed into the Sylgard bottom of the recording chamber. The continuous line is the detection threshold $\Phi = \sigma_n\sqrt{2\ln(f_c/\lambda_f)}$, where σ_n is the r.m.s. noise and λ_f is the error rate set to 0·1 s^{-1} (Colquhoun & Sigworth 1995, p. 495).

membrane patch without channel activity, but Sylgard seals are customary test objects. The continuous line in Fig. 1*C* shows the detection threshold (Φ) at the respective frequency f_c and r.m.s. noise (σ_n), with an error rate due to noise of 0·1 s^{-1}. For instance at 100 Hz filter cut-off the threshold for detecting an opening (see Fig. 2*C*) is at 13 fA, and 20 fA channels could well be resolved. At 100 kHz, the respective threshold would be at 17 pA.

RESULTS

The quality of the high time-resolution recordings and the conditions of evaluation of kinetic data are demonstrated in Fig. 2. In the original recordings with 78 kHz filter cut-off (blue) in Fig. 2*A*, two channel openings with 7 μs (arrows) and 70 μs durations were followed by a long opening. When the trace was filtered with 20 kHz filter cut-off (green) the very short opening was barely discernible, and it was lost with 5 kHz filter cut-off; 5 kHz was the filter cut-off in Colquhoun & Sakmann (1985) in which the closings within bursts were defined. In Fig. 2*B*, 2×10^{-3} M ACh elicits a burst broken up by ten short closings probably due to channel block by the high ACh concentration (Sine & Steinbach, 1987; Colquhoun & Ogden, 1988). At 5 kHz filter cut-off the closings were not resolved and apparently channel current amplitude was reduced with a relatively noisy open channel.

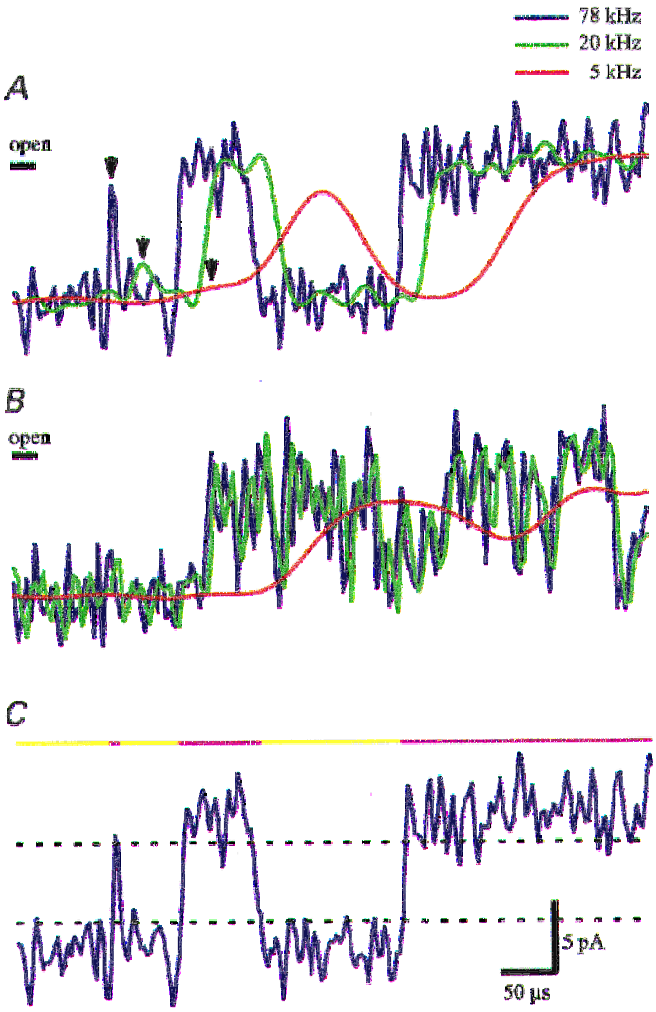

Figure 2. Single channel patch clamp currents recorded on-cell from mouse myotubes with 10^{-5} M ACh (*A* and *C*, same records) and 2×10^{-3} M ACh (*B*)

Polarization, −200 mV; 21 °C. The blue traces are filtered with a 78 kHz low pass filter, the green ones with a 20 kHz filter and the red ones with a 5 kHz filter. The 'open' level (bar) corresponds to 9·5 pA. *B*, 2×10^{-3} M ACh elicits a burst broken up by ten short closings due to channel block by the high ACh concentration. At 5 kHz filter cut-off the closings are not resolved and apparently channel current amplitude is reduced with a relatively noisy open channel. *C* explains the evaluation of current traces. A dashed upper threshold line is placed at 0·8 full amplitude at the lower margin of the open channel trace; when the current passes this upper threshold coming from the closed state, the program detects a channel opening. Vice versa, passing of the lower threshold at 0·2 full amplitude terminates the open state and a closure is detected. The program stores the time sequence of openings and closures as an 'idealized trace' shown above. The duration of a specific opening or closure is determined at half-amplitude.

Our 78 kHz filter cut-off recordings do not show sublevels of openings or closings. Figure 2*C* explains the evaluation of current traces. A dashed upper threshold line was placed at the lower margin of the open channel trace; when the current passed this upper threshold coming from the closed state, the program detected a channel opening. Vice versa, passing of the lower threshold terminated the open state and a closure was detected. The program stored the time sequence of openings and closures as an 'idealized trace' shown above. The duration of a specific opening or closure was determined at half-amplitude. These evaluations must contain some errors, since noise spikes may pass a threshold and generate a spurious opening or closure. As derived by Colquhoun & Sigworth (1995), the frequency of false events is proportional to the filter cut-off frequency and a function of Φ/σ_n, in which Φ is the detection threshold and σ_n the r.m.s. value of the noise (see Fig. 1*C*). In the case of Fig. 2*C*, the relative threshold Φ/σ_n was 5, which resulted in a false event rate of $0{\cdot}4\ s^{-1}$. Except for recordings below 10^{-6} M ACh, the rate of detected events was above $10^4\ s^{-1}$ in our data (see Fig. 3), and compared with this rate that of the false events was negligible. With ACh concentrations below 10^{-6} M the detected events had a rate around $100\ s^{-1}$, and 0·4 false events per second were acceptable. The predicted low error rates were verified also by evaluating 'negative openings', i.e. noise spikes crossing a threshold at 0·8 open amplitude set negative to the mean closed amplitude. The relatively noisy recordings presented here thus did not lead to appreciable errors of evaluation and further filtering would have destroyed information. With 78 kHz external filtering, the shortest event that was tested to reach full amplitude was 6 μs, and this limited the detection of signals.

Evaluations of channel open and closed times from traces like those in Fig. 2 were plotted as distributions of events per time bin. Figure 3 gives an example for an experiment with an ACh concentration of 10^{-5} M, with 3 μs bin width. The open time distribution contained three exponential components with the time constants or mean durations $\tau_{O1} = 1{\cdot}4\ \mu s$, $\tau_{O_2} = 36\ \mu s$ and $\tau_{O3} = 729\ \mu s$. τ_{O1} was shorter than any mean open time measured so far, but represents the largest component of the distribution, containing 0·94 of the total area. This component is shown in more detail in the inset of Fig. 3 (upper panel), presenting the first 30 μs of the distribution. The first bin, from 0 to 3 μs, was empty, since openings of less than 3 μs duration could not be resolved. The next bin bordered on the 6 μs minimum pulse duration to reach threshold, and some shorter pulses passed this threshold due to noise. However, the number of events was much reduced by filtering, and this bin was excluded from evaluation. For the third bin, from 6 to 9 μs, all events could have been resolved; if anything a small proportion were lost. Therefore, the fit started from 6 μs and the resulting 1·4 μs first component of the openings should be little distorted by the limited frequency resolution of the measurement. It should be noted that the distribution contained less than a hundredth of this first component; the rest was cut off in the first two bins due to filtering.

The closed times present the components $\tau_{C1} = 18\ \mu s$ and $\tau_{C2} = 79\ \mu s$; further components were much longer and depended on the number of channels present in the patch. Again the shortest component, τ_{C1}, was the largest, containing 0·51 of the area, while τ_{C2} amounted to 0·21. As shown in the inset of Fig. 3 (lower panel), this fit (thick line) started only from the fourth bin, 9–12 μs. Although closings longer than 6 μs should have been resolved, the third bin was not included in the fit, because solely its amplitude deviated from the 18 μs fit. If the third bin was included, a first short component $\tau'_{C0} = 1{\cdot}05\ \mu s$ was found, with $\tau'_{C1} = 19{\cdot}3\ \mu s$, insignificantly longer than τ_{C1}. The amplitude of τ'_{C0} was a thousand times larger than that of τ'_{C1} or τ_{C1}, and thus most of the possible 1·05 μs component of the closed times did not show up in the distribution of Fig. 3*B*. We think that this possible component can only be accepted when the time resolution has been further improved. Also Colquhoun & Sakmann (1985) mention indications of a very short additional closed time component in frog muscle. The omission of the very short closings imposes inconsistent different time resolutions on openings and closings (see Colquhoun & Sigworth 1995), but if the third bin was also disregarded in the open times, τ_{O1} remained unchanged.

The distributions of Fig. 3 are typical examples for the results of nine experiments at an ACh concentration of 10^{-5} M. In this concentration range, all distributions showed the same components, although at different amplitudes. The shortest open component predominated, containing on average 0·94 of the total charge, and had a mean duration of $1{\cdot}24 \pm 0{\cdot}72\ \mu s$ (mean $\pm$ standard deviation). The longer components, $\tau_{O_2} = 24{\cdot}7 \pm 14{\cdot}6\ \mu s$ and $\tau_{O3} = 790 \pm 420\ \mu s$, each contained about 0·025 of the total charge. Of the closed times, the shorter had a mean duration of $\tau_{C1} = 16{\cdot}4 \pm 6{\cdot}8\ \mu s$ and contained about half of the total area of the distribution, while $\tau_{C2} = 154 \pm 110\ \mu s$ contained 0·26 of the total area. In all closed time distributions the fit started only from 9 μs, ignoring a possible τ'_{C0} component.

For low ACh concentrations and nicotinic channels of adult frog muscle, Colquhoun & Sakmann (1985) have derived a reaction scheme which is extended here by the state A_1O_s and by a blocked state A_2BA which is filled only with ACh concentrations larger than 10^{-5} M (Scheme 1).

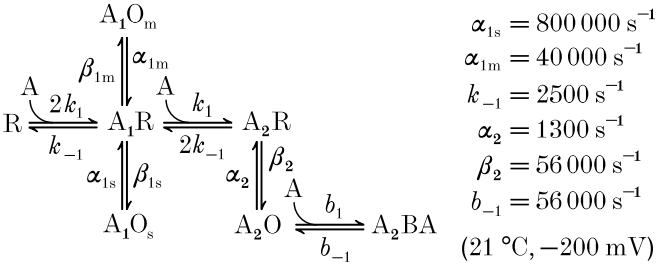

Scheme 1

R is the non-liganded receptor/channel, A the agonist ACh at the respective concentration, and O the open states which

arise from A_1R or A_2R as conformation changes. This scheme disregards the relatively slow desensitization reactions (Franke *et al.* 1992; Franke *et al.* 1993). How can we find out which open time components are associated with which closed times, how the ACh concentration affects such associations and to which of the rate constants in Scheme 1 they are related? Magleby & Weiss (1990) have suggested plotting two-dimensional distributions of closed times *versus* the following open time. Peaks in these two-dimensional distributions identify specific relations within the reaction scheme. Data from experiments with 10^{-7}, 10^{-6} and 10^{-5} M ACh are plotted in the left-hand column of Fig. 4. In all three graphs a red/green peak lies close to 10 μs open time. The centre of this peak certainly is below 6 μs open time, since below 10 μs the openings are cut down by the filter. We can associate this peak with $\tau_{O1} = 1{\cdot}24$ μs of the open time distributions. We see that τ_{O1} with 0·1–10 μM ACh is associated with long closed times of

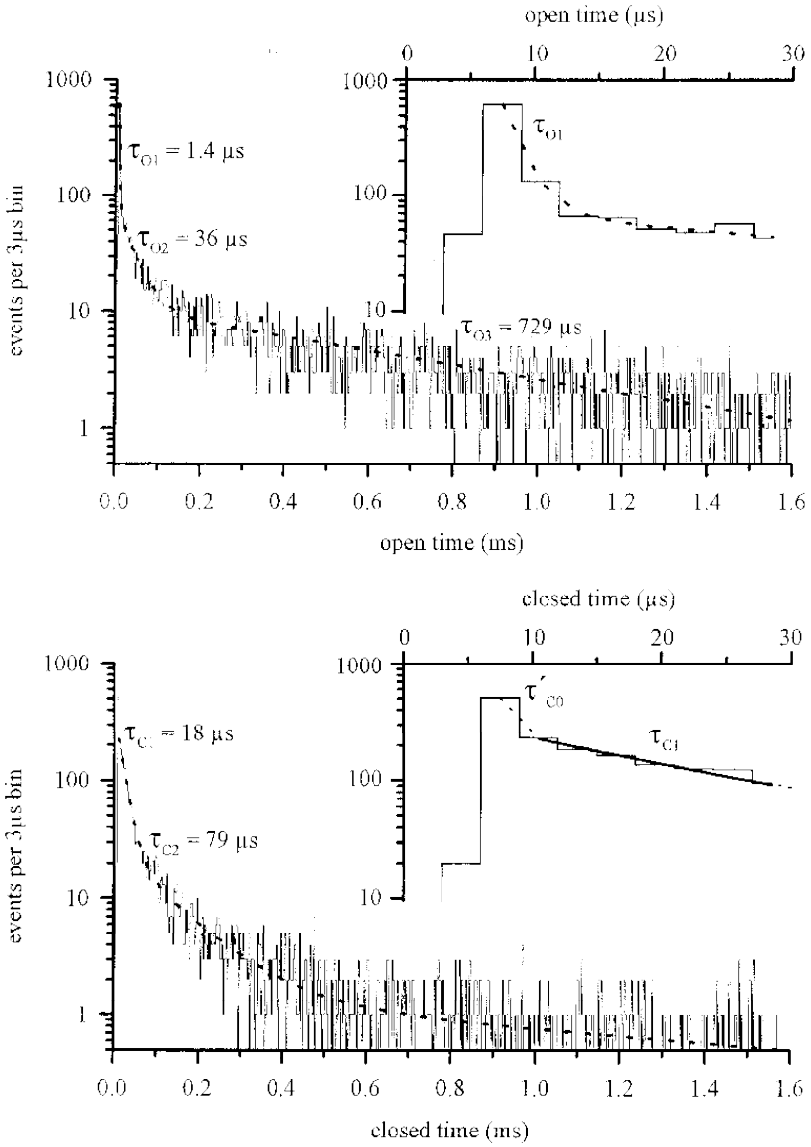

Figure 3. Distributions of open times and closed times for one experiment with 10 μM ACh

Insets show the first ten bins. The open time distribution contains three exponential components with the time constants or mean durations $\tau_{O1} = 1{\cdot}4$ μs, $\tau_{O_2} = 36$ μs and $\tau_{O3} = 729$ μs. τ_{O1} represents by far the largest component of the distribution, containing 0·94 of the total area. The closed times present the components $\tau_{C1} = 18$ μs and $\tau_{C2} = 79$ μs; further components are much longer and depend on the number of channels present in the patch. Again the shortest component τ_{C1} is the largest, containing 0·51 of the area, while τ_{C2} amounts to 0·21. As shown in the inset this fit (thick line) starts only from the fourth bin, 9–12 μs. Although closings longer than 6 μs should have been resolved, the third bin was not included in the fit, because solely its amplitude deviates from the 18 μs fit. If the third bin is included, a first short component $\tau'_{C0} = 1{\cdot}05$ μs is found (dotted line).

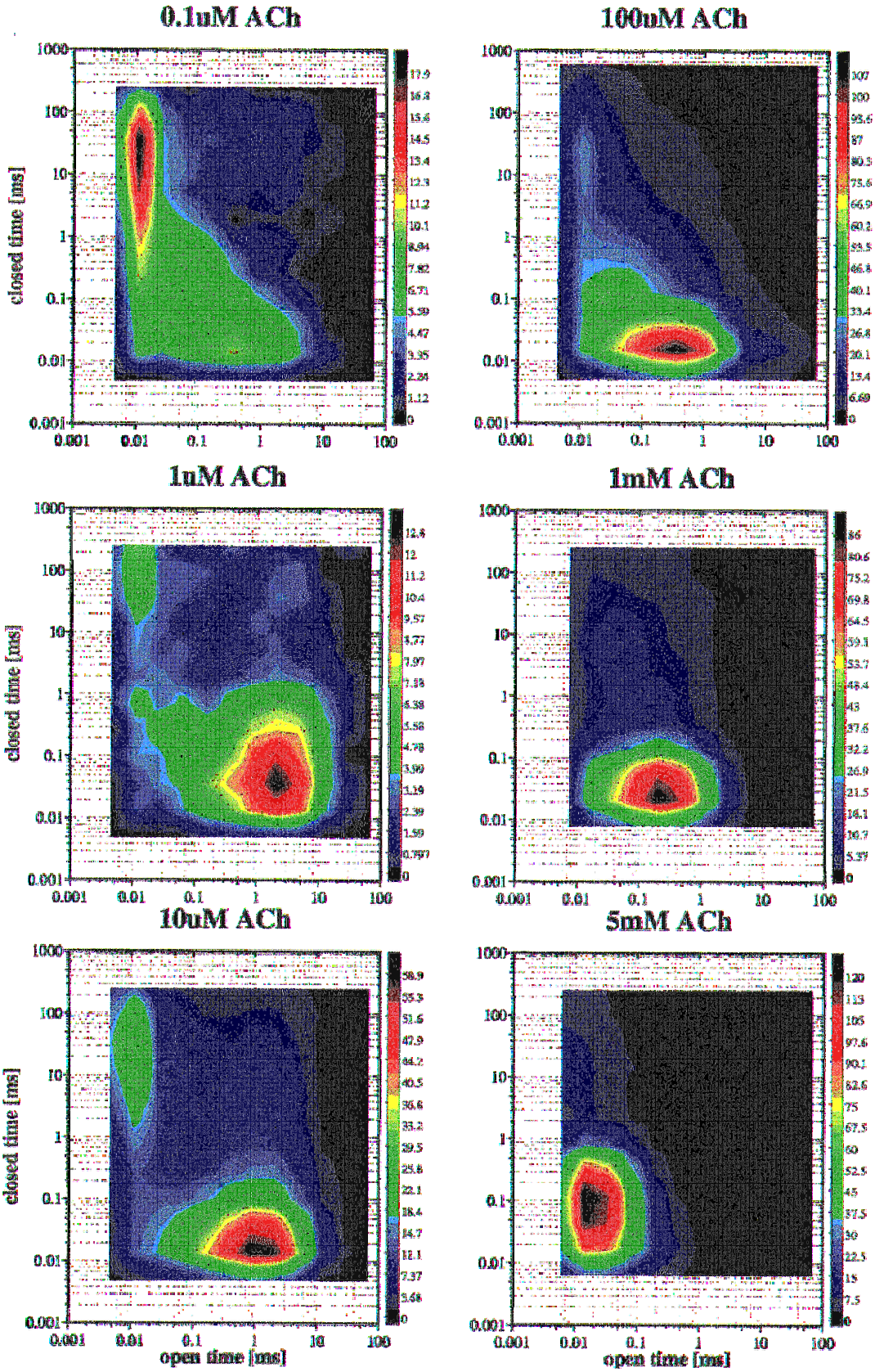

Fig. 4. For legend see facing page.

1–100 ms; these very short openings thus are single spikes like the 7 μs opening in Fig. 2*A*. A second prominent peak with 0·1–10 μM ACh represents an open time of about 1 ms and corresponds to $\tau_{O3} = 0{\cdot}8$ ms of the one-dimensional distributions. These long openings were preceded by short closures of about 20 μs duration, corresponding to $\tau_{C1} = 16$ μs. The peak at the lower right thus represents bursts of on average 0·8 ms openings alternating with 16 μs closures. This peak was higher with 10 μM ACh than with 1 μM ACh, and almost disappeared with 0·1 μM ACh. Vice versa the very short open time peak declined in amplitude with rising ACh concentration. The state of the channel generating the single short openings was therefore predominantly occupied at low ACh concentrations and may be represented by the state A_1O_s in Scheme 1, while the bursts with long openings and short closures represent oscillations between the higher liganded A_2R and A_2O states. We are left with the relatively small components $\tau_{O_2} = 25$ μs and $\tau_{C2} = 154$ μs, which may refer to a weak peak in the green region between the two peaks with 0·1–1 μM ACh. This peak, like that of the single short openings, decreased on increasing the ACh concentration and may be associated with the state A_1O_m in Scheme 1.

From the lifetimes of the different open and closed states and the burst duration (mean, 10·0 $\pm$ 5·5 ms) the rate constants α_{1s} to β_2 can be calculated (Colquhoun & Hawkes 1982; Colquhoun & Sakmann 1985); they are given in Scheme 1.

In the right-hand column of Fig. 4 the ACh concentration increases from 0·1 to 5 mM. Aside from the remnants of short openings in the upper left panel, there is only the 'burst' peak. Relative to its open time centred on approximately 1 ms with 10 μM ACh, the centre of the burst peak shifts little with 0·1 mM ACh, to 0·2 ms with 1 mM ACh, and to about 20 μs open time with 5 mM ACh. Simultaneously, there is little change in the closed times within the bursts; in distributions such as that in Fig. 3 the τ_{C1} component became 18 μs on average between 0·1 and 5 mM ACh, which is almost the same as the closed times $\tau_{C1} = 16$ μs in the low ACh-concentration bursts (see also Fig. 2*B*). At higher ACh concentrations, the open state A_2O (with the basic lifetime of 800 μs) is interrupted by binding of ACh creating the closed state A_2BA (Scheme 1), by 'open channel block'. The mean duration of these blocks of 18 μs is the lifetime of the A_2BA state, and 1/18 μs corresponds to the rate $b_{-1} = 56\,000$ s^{-1} in Scheme 1. With 5 mM ACh in Fig. 4 the open state lasts only about 20 μs. The lifetime of A_2O with high ACh concentrations is $\tau'_{01} = (\alpha_2 + A \cdot b_1)^{-1}$, and for 5 mM ACh results a blocking rate constant b_1 of about 10^7 M^{-1} s^{-1}.

While with up to 1 mM ACh in Fig. 4 the closed times of the 'bursts' are in the 20 μs range of τ_{C1}, with 5 mM ACh the peak extended to 100 μs closed times. In one-dimensional distributions like Fig. 3, but for 5 mM ACh, in addition to the usually predominant component τ_{C1} a mean $\tau_{C2} = 72$ μs appeared which had double the amplitude of τ_{C1}. τ_{C2} probably represents a second, longer component of open channel block.

DISCUSSION

The main result of the present study is the demonstration that patch-clamp current recordings from single channels are possible and fruitful at filter frequencies of 78 kHz with a defined and acceptable error rate, pushing the detection limit for openings or closings to 6 μs. The actual limit is not even set by the noise, but by the rate of digitalization of 333 kHz. Analog–digital converters storing continuously at higher rates are not available at present; 1–5 MHz analog–digital converters will be on the market soon, and also further improvements of the quartz electrodes seem possible. Aside from the necessity of a suitable quartz-glass puller, the low noise technique is hardly more complicated than standard recordings. There seems to be one disadvantage: apparently patches on quartz glass are less stable than those on borosilicate glass. Certainly the technique is applicable and useful also for other channel types, for instance for glutamatergic channels with very short open times, or for channels with current amplitudes down to 20 fA for which single channel currents have not been resolved so far (see Fig. 1*C*).

We have demonstrated the usefulness of this technique at the most thoroughly investigated channel type, the neuromuscular nicotinic channel. For this channel we could improve the kinetic activation rate constants (see Scheme 1) and we have found a new extremely short type of, on average, 1·2 μs openings. We have taken the τ values from the distributions without correcting them for missing events (Colquhoun & Hawkes 1995). It is clear, for instance, that

Figure 4. Correlations of closed times (ordinates) with the following open time (abscissae) from idealized traces as in Fig. 2*C*

The square root of the number of events per log-bin is represented by the colour code at the right. In the left panel the ACh concentration rises from 0·1 to 10 μM. At 0·1 μM ACh, there is one peak containing open times around 10 μs and multiple relatively long closed times. With increasing ACh concentrations, this peak becomes weaker and a peak around 1 ms open time and 20 μs closed times grows. The first peak represents τ_{O1}, short single openings of singly liganded receptors, while the second peak is generated by burst of 800 μs openings (τ_{O3}) with 16 μs closings (τ_{C1}) of the doubly liganded receptors. In the right panel with 0·1–5 mM ACh, the 'burst' peak shifts more and more towards shorter open times; the 800 μs openings are interrupted by 18 μs closings due to binding of ACh to open channels (see Fig. 2*B*). With 5 mM ACh the peak extends to closed times of 400 μs, indicating a second, longer component of open channel block.

the 800 μs open times measured within a burst would be shortened if closings of less than 6 μs could also be resolved. Since we still see the possibility of improving the time resolution of the measurements, calculatory corrections will be left to a future study.

In previous studies of single embryonic mouse muscle channels, lower rates of conformational changes than those in Scheme 1 have been measured, obviously due to insufficient time resolution (Franke *et al.* 1992, 1993; Zhang *et al.* 1995). The rates k_{-1}, α_2 and β_2 have also been deduced from the rising phases of channel currents elicited by pulses of ACh directed to outside-out patches (Franke *et al.* 1991), and again the α_2 and β_2 were too low compared with the present results. A recent study of Maconochie & Steinbach (1998) improved this method and derived a $\beta_2 = 60\,000$ s^{-1} for recombinant fetal receptors, which agrees with the value found here. Previous studies have also seen openings in the 100 μs range from monoliganded channels, which are probably equivalents of our A_1O_m state. Our much larger A_1O_s component with 1·2 μs mean open time could not have been detected with at best 5 kHz filtering.

Jackson (1988) has reported for mouse muscle not only 1·1 ms openings from the single liganded receptors, but 40 times less frequent 0·2 ms openings from non-liganded ones. In our preparation openings without ACh application have never been seen (Franke *et al.* 1992, 1993), but this is negative evidence. However, our results seem to exclude the possibility that the components A_1O_s or A_1O_m might have been generated by the unliganded receptor. The proportions of amplitudes of A_1O_s and A_1O_m remain almost constant from 10^{-7} to 10^{-4} M ACh; if one of the short opening components would arise from R, its amplitude relative to an A_1O component should fall almost reciprocal to ACh concentration.

The two-threshold crossing detection method that is used here is appropriate for the present data. However, if the records contain a significant proportion of sublevel events, it may be necessary to apply 'time-course fitting' (Colquhoun & Sigworth 1995, program at http://www.ucl.ac.uk/Pharmacology/dc.html).

Benndorf, K. (1994). Properties of single cardiac Na channels at 35 °C. *Journal of General Physiology* **104**, 801–820.

Benndorf, K. (1995). Low-noise recording. In *Single-Channel Recording*, 2nd edn, ed. Sakmann, B. & Neher, E., pp. 129–145. Plenum Press, New York.

Colquhoun, D. & Hawkes, A. G. (1982). On the stochastic properties of bursts of single ion channel openings and of clusters of bursts. *Philosophical Transactions of the Royal Society* B **300**, 1–59.

Colquhoun, D. & Hawkes, A. G. (1995). The principles of the stochastic interpretation of ion-channel mechnanisms. In *Single-Channel Recording*, 2nd edn, ed. Sakmann, B. & Neher, E., pp. 397–479. Plenum Press, New York.

Colquhoun, D. & Ogden, D. C. (1988). Activation of ion channels in the frog end-plate by high concentrations of acetylcholine. *Journal of Physiology* **395**, 131–159.

Colquhoun, D. & Sakmann, B. (1985). Fast events in single-channel currents activated by acetylcholine and its analogues at the frog muscle end-plate. *Journal of Physiology* **369**, 501–557.

Colquhoun, D. & Sigworth, F. J. (1995). Fitting and statistical analysis of single-channel records. In *Single-Channel Recording*, 2nd edn, ed. Sakmann, B. & Neher, E., pp. 483–585. Plenum Press, New York.

Franke, Ch., Hatt, H., Parnas, H. & Dudel, J. (1991). Kinetic constants of the acetylcholine (ACh) receptor reaction deduced from the rise in open probability after steps in ACh concentration. *Biophysical Journal* **60**, 1008–1016.

Franke, Ch., Költgen, D., Hatt, H. & Dudel, J. (1992). Activation and desensitization of embryonic-like receptor channels in mouse muscle by acetylcholine concentration steps. *Journal of Physiology* **451**, 145–158.

Franke, Ch., Parnas, H., Hovav, G. & Dudel, J. (1993). A molecular scheme for the reaction between acetylcholine and nicotinic channels. *Biophysical Journal* **64**, 339–356.

Hamill, O. P., Marty, A., Neher, E., Sakmann, B. & Sigworth, F. J. (1981). Improved patch-clamp techniques for high-resolution current recording from cells and cell-free membrane patches. *Pflügers Archiv* **391**, 85–100.

Jackson, M. B. (1988). Dependence of acetylcholine receptor channel kinetics on agonist concentration in cultured mouse muscle fibres. *Journal of Physiology* **397**, 555–583.

Levis, R. A. & Rae, J. L. (1993). The use of quartz patch pipettes for low noise single channel recording. *Biophysical Journal* **65**, 1666–1677.

Maconochie, D. J. & Steinbach, J. H. (1998). The channel opening rate of adult- and fetal-type mouse muscle nicotinic receptors activated by acetylcholine. *Journal of Physiology* **506**, 53–72.

Magleby, K. L. & Stevens, C. F. (1972). A quantitative description of end-plate currents. *Journal of Physiology* **223**, 173–197.

Magleby, K. L. & Weiss, D. S. (1990). Identifying kinetic gating mechanisms for ion channels by using two-dimensional distributions of simulated dwell times. *Proceedings of the Royal Society* B **241**, 220–228.

Neher, E. & Steinbach, J. H. (1978). Local anaesthetics transiently block currents through single acetylcholine-receptor channels. *Journal of Physiology* **277**, 153–176.

Sine, S. M. & Steinbach, J. H. (1987). Activation of acetylcholine receptors on clonal mammalian BC3H-1 cells by high concentrations of agonist. *Journal of Physiology* **385**, 325–359.

Zhang, Y., Chen, J. & Auerbach, A. (1995). Kinetics of wild-type, embryonic nicotinic acetylcholine receptors activated by acetylcholine, carbamylcholine, and tetramethyl-ammonium. *Journal of Physiology* **481**, 189–206.

Acknowledgements

We thank Mr D. Beyer and W. Zeitz for skilful assistance in developing the quartz glass puller and modifying the head stage, Miss M. Hammel for preparing the cell cultures and Mrs M. Griessl for secretarial help. The scanning electron-microscopic images were expertly prepared by Dr J. Tomczok, Dermatologische Klinik des Klinikums rechts der Isar, Technische Universität München. Supported by the Deutsche Forschungsgemeinschaft.

Corresponding author

J. Dudel: Institut für Physiologie, Technische Universität München, Biedersteiner Strasse 29, D-80802 Munich, Germany.

Email: dudel@physiol.med.tu-muenchen.de